J. Biochem. 124, 634-641 (1998)

Roles of the Ser146, Tyr159, and Lys163 Residues in the Catalytic Action of 7α-Hydroxysteroid Dehydrogenase from *Escherichia coli*[1]

Tetsurou Tanabe,* Nobutaka Tanaka,† Kouichiro Uchikawa,* Tsutomu Kabashima,* Kiyoshi Ito,* Takamasa Nonaka,‡ Yukio Mitsui,‡ Masato Tsuru,§ and Tadashi Yoshimoto*,[2]

**School of Pharmaceutical Sciences, Nagasaki University, 1-14 Bunkyo-machi, Nagasaki 852-8521; †School of Pharmaceutical Sciences, Showa University, 1-5-8 Hatanodai, Shinagawa-ku, Tokyo 142-8555; ‡Department of BioEngineering Nagaoka University of Technology, Kamitomioka, Nagaoka, Niigata 940-2137; and §Information Science Center, Nagasaki University, 1-14 Bunkyo-machi, Nagasaki 852-8521*

Received for publication, May 6, 1998

The *Escherichia coli* 7α-hydroxysteroid dehydrogenase (7α-HSDH; EC 1.1.1.159) has been the subject of our studies, including the cloning of its gene, and determination of the crystal structures of its binary and ternary complexes [*J. Bacteriol.* 173, 2173-2179 (1991); *Biochemistry* 35, 7715-7730 (1996)]. Through these studies, the Ser146, Tyr159, and Lys163 residues were found to be involved in its catalytic action. In order to clarify the roles of these residues, we constructed six single mutants of 7α-HSDH, Tyr159-Phe (Y159F), Tyr159-His (Y159H), Lys163-Arg (K163R), Lys163-Ile (K163I), Ser146-Ala (S146A), and Ser146-His (S146H), by site-directed mutagenesis. These mutants were overexpressed in *E. coli* WSD, which is a 7α-HSDH null strain, and the expressed enzymes were purified to homogeneity. The kinetic constants of the mutant enzymes were determined, and the structures of the Y159F, Y159H, and K163R mutants were analyzed by X-ray crystallography. The Y159F mutant showed no activity, while the Y159H mutant exhibited 13.3% of the wild-type enzyme activity. No remarkable conformational change between the Y159F (or Y159H) and wild-type proteins was detected on X-ray crystallography. On the other hand, the K163I mutant showed just 5.3% of the native enzyme activity, with a 8.5-fold higher K_d. However, the K163R mutant retained 64% activity, and no remarkable conformational change was detected on X-ray crystallography. In the cases of the S146A and S146H mutants, the activities fairly decreased, with 20.3 and 35.6% of k_{cat} of the wild-type, respectively. The data presented in this paper confirm that Tyr159 acts as a basic catalyst, that Lys163 binds to NAD(H) and lowers the pK_a value of Tyr159, and that Ser146 stabilizes the substrate, reaction intermediate and product in catalysis.

Key words: catalytic mechanism, site-directed mutagenesis, steroid dehydrogenase, X-ray analysis.

The *Escherichia coli* 7α-HSDH, which acts on the hydroxyl group at position 7 of the steroid skeleton of bile acids, has been the subject of many studies since its finding and isolation (*1, 2*). Yoshimoto *et al.* have cloned, sequenced and characterized the enzyme gene, finding it to comprise 765 bp, and to code for a protein of a molecular weight of 26,778 (*3, 4*). Based on the deduced amino acid sequence, the enzyme was classified as a member of the short-chain dehydrogenase/reductase (SDR) family (*3*). The enzymes belonging to this family exhibit wide substrate specificities for alcohol, ribitol, glucose, 15-hydroxyprostaglandin and several hydroxysteroids. To date, more than 50 different members have been characterized (*5*).

Recently, the crystal structures of the 7α-HSDH binary and ternary complexes (complexed with NAD^+, and NADH and 7-oxoglycochenodeoxycholic acid, respectively) were resolved by X-ray crystallography by Tanaka *et al.* (*6*). The crystal structure of the ternary complex of 7α-HSDH was the first one described for an enzyme of the SDR family. This structure provided firm evidence that Tyr159 and Ser146, which are highly conserved in the SDR family, directly interact with the hydroxyl group of substrates/products, and also suggested that the strictly conserved Lys163 residue plays two critical roles: interaction with the 2′- and 3′-hydroxyl groups of the nicotinamide ribose (cofactor binding), and lowering of the pK_a value of the hydroxyl group of the conserved tyrosine residue. The studies on the respective mutants described in this paper made it possible to further study the roles of the Tyr159, Ser146, and Lys163 residues in the catalytic mechanism of 7α-HSDH.

[1] This work was supported in part by a Grant-in-Aid for Scientific Research from the Ministry of Education, Science, Sports and Culture of Japan.

[2] To whom correspondence should be addressed. E-mail: t-yoshimoto@cc.nagasaki-u.ac.jp

Abbreviations: HSDH, hydroxysteroid dehydrogenase; SDR, short-chain dehydrogenase/reductase; ODA, oligonucleotide-directed dual amber; GCDCA, glycochenodeoxycholic acid; PEG, polyethylene glycol; CA, cholic acid.

MATERIALS AND METHODS

Materials—Restriction endonucleases, other modification enzymes, a GeneAmp^R PCR reagent kit, and a Mutan^R-Super Express Km kit were purchased from Takara Shuzo and New England Bio Labs. NAD^+ was from Kojin Kagaku. Polyethylene glycol with a mean molecular weight of 6000 (PEG6000) was purchased from Nacalai Tesque. The oligonucleotide primers containing the desired changes for the mutants were synthesized by Takara Shuzo.

Bacterial Strains and Plasmids—*E. coli* MV1184 (*ara*, Δ(*lac-proAB*), *rpsL*, *thi* (*f*80*lac*ΔM15), Δ(*srl-recA*)306::Tn*10*(*tet*^{r})/F$'$[*traD*36, *proAB*$^+$, *lac Iq*, *lacZ*ΔM15]), DH1 (*supE*44, *hsdR*17, *recA*1, *endA*1, *gyrA*96, *relA*1, *thi*-1), W3110 [λ$^-$, in (*rrn*D-*rrn*E)], and a W3110 mutant [*rec*D::Tn*10* (tet^r)] were used for site-directed mutagenesis. Plasmids pUC19, pKF18k, and pUC118 were used as vectors.

Inactivation of the 7α-HSDH Gene in E. coli W3110—To inactivate the 7α-HSDH gene in the host strain (*E. coli*), a disrupted 7α-HSDH mutant in *E. coli* W3110 was constructed by the P1 transduction method as follows,

(1) Homologous Recombination—A 1.2 kbp DNA fragment harboring the complete aminoglycoside 3′-phospho transferase gene (Km^r) was inserted in the *Eco*T22I site of pSD3, which was constructed by insertion of a 1.8 kbp *Bam*HI-*Pst*I fragment of the 7α-HSDH gene into pUC118, resulting in pSD3Km. *E. coli* W3110 mutant [*rec*D::Tn*10* (tet^r)] was transformed with the 3.0 kbp *Bam*HI/*Pst*I restriction fragment of plasmid pSD3Km.

(2) Isolation of a P1kc Phage Lysate of the W3110 Mutant—The mutant strain [*rec*D::Tn*10* *hsd*::Km] was grown in 2 ml of LB-broth containing 25 μg/ml kanamycin and 15 μg/ml tetracycline at 37°C until $OD_{600} = 0.3$. After 0.2 ml of the cultured cells had been transferred to a new tube, 20 μl of P1*kc* phage and 2.5 ml of soft agar (LB-broth containing 0.5% glucose, 2 mM $CaCl_2$, and 0.7% agar) at 48°C were added. The cultured cells were poured onto an LB plate and then incubated overnight at 37°C. Three milliliter of LB-broth and 50 μl of chloroform were added to the LB plate, which was then kept at 4°C for 3 h. The LB-broth containing the P1*kc* phage was transferred to a new tube, 70 μl of chloroform was added, and then the mixture was mixed gently. The supernatant isolated on centrifugation was used as the P1*kc* phage lysate carrying *hsd*::Km.

(3) Generalized P1 Transduction—*E. coli* W3110 (wild type) was grown in 2 ml of LB-broth at 37°C until $OD_{600} = 0.3$. One milliliter of the cultured cells was transferred to a new tube. The cells were harvested, washed twice with 1 ml of LB-broth containing 0.5% glucose and 2 mM $CaCl_2$, and then suspended in 1 ml of the same broth. After the addition of 0.1 ml of P1*kc* phage lysate carrying *hsd*::Km, the culture was kept at room temperature for 1 h. The cells were then harvested and resuspended in 0.1 ml of LB-broth. The culture was spread onto an LB plate containing 30 μg/ml kanamycin and then incubated overnight at 37°C. The selected strain, *E. coli* W3110 [*rec*D::Tn*10* *hsd*::Km], which was called WSD, was used as the host to express mutant genes (*7, 8*).

Construction of a Site-Directed Mutant Gene—The ODA and PCR methods were used for the construction of the six mutants; the former for Y159F and Y159H, and the latter for K163R, K163I, S146A, and S146H.

1) A Mutan^R-Super Express Km kit based on the oligonucleotide-directed dual amber (ODA) method (*9*) was used. Plasmid pSD3 was digested with *Taq*I and *Bam*HI, and pKF18k was digested with *Acc*I and *Bam*HI, and then these were ligated. Then the constructed plasmid, designated as pSD3KF1, was used to transform *E. coli* DH1 by the $RbCl_2$-$CaCl_2$ method (*10*).

PCR was carried out in a 50 μl reaction mixture comprising 5 pmol selection primer, 5 pmol mutagenized primer, 10 ng of template DNA, 5 μl of 10×LA PCR Buffer II (Mg^{2+} plus), 8 μl of a dNTP mixture, 2.5 mM each, and 2.5 units of TAKARA LA Taq™ DNA polymerase. The amplification conditions consisted of 30 cycles of denaturation at 94°C for 1 min, annealing at 50 or 55°C for 1 min, and extension at 72°C for 3 min. After the PCR cycles, the reaction mixture was allowed to cool to 4°C.

The DNA in the reaction mixture was precipitated by adding 25 μl of 4 M ammonium acetate and 100 μl of 100% cold ethanol. The precipitate was washed twice with 70% ethanol, dried under vacuum, and then dissolved in 5 μl of sterilized water. This DNA solution containing plasmid DNA was used to transform *E. coli* MV1184, and the transformants were selected on an LB plate containing 50 μg/ml kanamycin. Mutations were confirmed by sequence analysis. DNA fragments containing individual mutations were prepared by digesting the respective plasmids with *Bam*HI and *Nru*I. These fragments were cloned into *Bam*HI and *Nru*I-digested plasmid pSD3, and then the cloned plasmids were used to transform *E. coli* WSD for expression.

2) The other method used included PCR amplification (*11*) with a GeneAmp^R PCR reagent kit. Plasmid pSD3 was digested with *Bam*HI and *Nru*I, and pUC19 was digested with *Bam*HI and *Hinc*II, and then these were ligated. Then the constructed plasmid, pSD3C1, was used to transform *E. coli* DH1.

PCR was carried out in a 100 μl reaction mixture comprising 100 pmol primer for mutation, 100 pmol T7 primer, 50 ng of template DNA, all four dNTPs, 0.1 mM each, 10 μl of 10× reaction buffer, and 2.5 units of AmpliTaq™ DNA polymerase. The amplification conditions consisted of 30 cycles of denaturation at 94°C for 1 min, annealing at 55°C for 1.5 min, and extension at 72°C for 2 min. After analysis of the PCR products on a 1.0% agarose gel, the amplified products were excised from the gel, followed by purification with QIAEX Gel Extraction Kits (QIAGEN).

The gel-purified primary PCR products and T3 primer were used for the second PCR, 30 cycles. After the mutations had been confirmed, the gel-purified second PCR products were digested with *Bam*HI and *Eco*T22I. The fragments containing mutations were cloned into *Bam*HI/*Eco*T22I-digested plasmid pSD3, and then the cloned plasmids were used to transform *E. coli* WSD. The primers used for mutation are shown in Table I.

Enzyme Activity Assay and Purification Methods—The enzyme activity was measured by the method of Yoshimoto *et al.* (*3*). The protein concentration was determined by the method of Bradford (*12*). The enzymes were purified by almost the same method as that of Yoshimoto *et al.* (*3*).

Cofactor Binding Studies—The fluorescence of the enzyme was measured at 25°C in 0.1 M sodium phosphate

buffer, pH 8.5. The excitation wavelength was 280 nm and the emission wavelength was 340 nm. The dissociation constants for NAD^+ were derived from the observed decrease in protein fluorescence on titration by adding an NAD^+ solution in volumes of 5 μl, based on the relationship outlined by Stinson and Holbrook (*13*), in which

$$K/1-a=[\text{ligand}]\text{total}/a-[E_o]$$

where a is the fractional saturation of ligand binding sites, E_o the total binding sites, and K the dissociation constant. The dissociation constant was calculated from the slope of a plot of $1/1-a$ against [ligand]total/a.

Preparation of Binary and Ternary Complex Crystals—Crystals of a binary complex with NAD^+ were obtained by the hanging drop vapor diffusion method using conditions similar to those employed for the crystallization of the wild-type 7α-HSDH (with called the native crystal) (*6, 14*). The droplet and reservoir solutions were buffered with 100 mM Tris (pH 8.5) and mixed in the ratio of 1:1. The protein solution contained 20-25 mg/ml enzyme and 4 mg/ml NAD^+. The reservoir solution contained 26 or 28% (w/v) PEG 6000 and 200 mM sodium acetate.

To obtain ternary complex crystals containing NADH and a substrate/product, the above-mentioned binary complex crystals were soaked for 2 days at 20°C in the substrate solution. This solution was buffered with 100 mM Tris (pH 8.5), and contained 30% (w/v) PEG 6000, 0.2 M sodium acetate, 2 mg/ml NAD^+, and 5 mM glycochenodeoxycholic acid (GCDCA) as the substrate.

X-Ray Data Collection and Processing—Before X-ray data collection, crystals of the binary complex were transferred from a hanging drop to a freshly prepared standard solution. This solution was buffered at pH 8.5 with 100 mM Tris containing 30% PEG 6000, 0.2 M sodium acetate, and 2 mg/ml NAD^+. X-ray data collection was performed by the oscillation method at 20°C using a Rigaku R-AXIS IIC area detector with graphite-monochromated CuKα radiation, which was generated by a Rigaku RU200 rotating-anode X-ray generator (operated at 40 kV and 100 mA). Each data set was processed with the program, PROCESS, installed in the R-AXIS IIc system. The conditions for data processing were essentially the same as those for the wild-type (*14*).

Model Building and Structure Refinement—The crystal structures of the mutants were solved by means of difference Fourier techniques with standard refinement procedures employing the program, X-PLOR (*15*), and using the wild-type 7α-HSDH structures of the binary and ternary complexes as the starting models. Verification of the mutated residues was performed with the combination of omit and difference maps calculated with X-PLOR and displayed with the program, TURBO FRODO. Difference maps also revealed water positions in the mutants for comparison with the wild-type water positions.

TABLE I. **Primers for mutagenesis.**

Mutants[a]	Oligonucleotides[b]
Tyr159-Phe (Y159F)	5′-TAGATGATGC<u>AAA</u>GGAAGTC-3′
Tyr159-His (Y159H)	5′-AGATGATGC<u>ATG</u>GGAAGTCAT-3′
Lys163-Arg(K163R)	5′-GCCGCAGC<u>TCT</u>AGATGATGC-3′
Lys163-Ile (K163I)	5′-GCCGCAGC<u>TAT</u>AGATGATGC-3′
Ser146-Ala (S146A)	5′-GCCGCCAT<u>AGC</u>AGTGATGGTC-3′
Ser146-His (S146H)	5′-GCCGCCAT<u>ATG</u>AGTGATGGTC-3′

[a]Numbers refer to amino acid positions in the wild type 7α-HSDH. [b]Mutated nucleotides are underlined.

RESULTS

Purification of the Mutant Enzymes—All the enzymes were purified from cell-free extracts of *E. coli* WSD as described under "MATERIALS AND METHODS." As shown in Fig. 1, the purified enzymes were homogeneous. The purification procedure was easy to perform and gave good yields. Typically, 100-200 mg of enzyme could be obtained from 12 liters of culture. All mutants, except Y159F, showed 7α-HSDH activity. The identities of the isolated mutant enzymes were confirmed on SDS-PAGE analysis by the appearance of a band at around 28 kDa corresponding to the wild-type enzyme.

Kinetic Analysis of the Wild-Type and Mutant Enzymes—The kinetic parameters of each mutant, including K_m for cholic acid and NAD^+, K_d for NAD^+, k_{cat}, and catalytic efficiency (k_{cat}/K_m), were determined (Table II).

In the crystal structure of the ternary complex of wild-type 7α-HSDH (*6*), the highly conserved Tyr159 and Ser146 residues directly interact with the oxygen atom at position 7 of the steroid skeleton of bile acid (Fig. 2). As shown in Table II, the Y159F mutant showed a complete loss of activity. This clearly indicates that the tyrosine residue is essential for catalysis. However, the Y159H mutant somewhat retained the activity, with 13.3% of the k_{cat}, and no change in the K_m for both substrates (cholic acid and NAD^+) or the K_d for NAD^+. The S146A and S146H mutants also showed fairly reduced activity, with 20.3 and 35.6% of the k_{cat}. The K_m values for both substrates were similar to those of the wild-type.

On the other hand, Lys163, which was hydrogen-bonded to the 2′,3′-hydroxyl groups of the nicotinamide ribose of NAD^+, was mutated to isoleucine and arginine. K163I showed an 8.5-fold higher K_d and only 5.3% of the k_{cat} of the wild-type enzyme. K163R is, however, more active when compared with the K163I mutant. The k_{cat} value decreased to 64% of that of the wild-type enzyme, the K_m values for both substrates were unchanged, and the K_d for NAD^+ was similar to that of K163I.

Crystallization and Data Processing—Of the six mutants, three have been crystallized and structurally char-

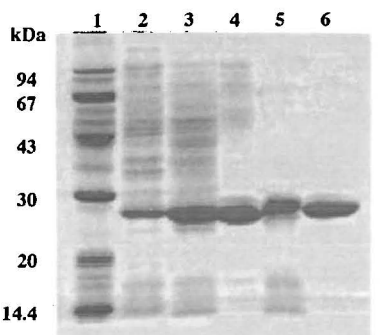

Fig. 1. **SDS-PAGE of purification of Y159F.** Lane 1, marker proteins; lane 2, cell-free extract; lane 3, protamine treatment; lane 4, ammonium sulfate fractionation, from 40 to 80%; lane 5, Toyopearl HW65C column chromatography; lane 6, DEAE-Toyopearl column chromatography.

acterized: Y159F, Y159H, and K163R. The best crystals of these mutants for data collection were obtained at different PEG concentrations: 25% for Y159F and Y159H, and 28% for K163R. All crystals belong to the same tetragonal space group as the wild-type enzyme crystal, $P4_12_12$. The sizes of the crystals were also similar; approximately $0.3 \times 0.3 \times 0.7$ mm^3, although there were slight differences in the cell dimensions (Table III).

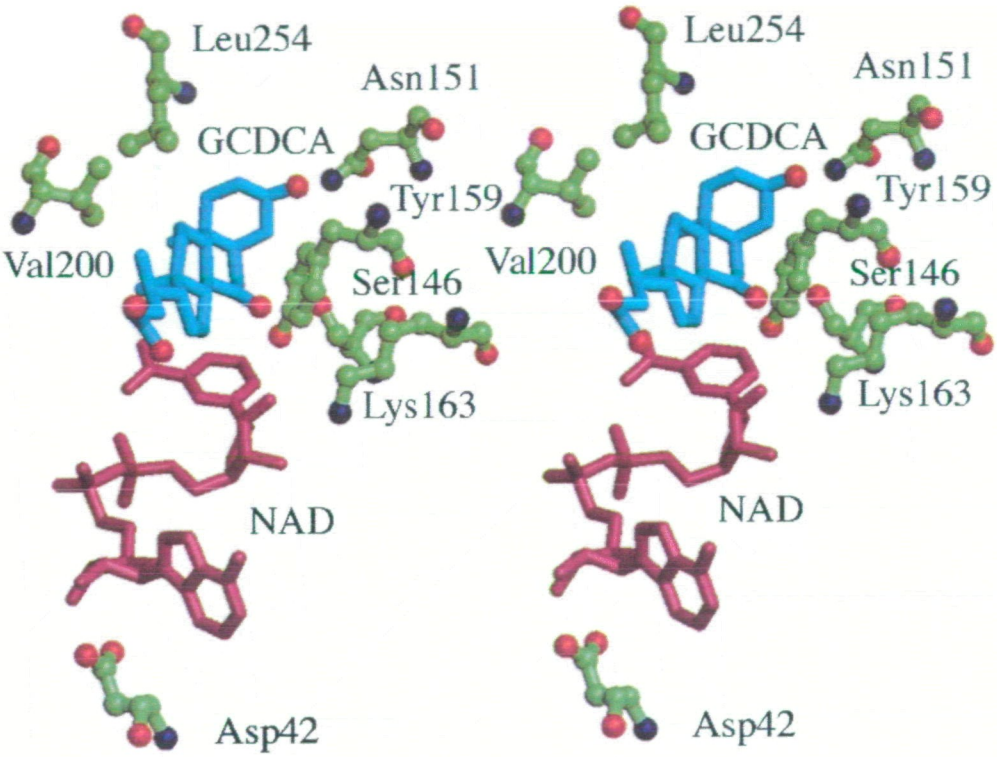

Fig. 2. **Stereoview of the active site in the ternary complex of 7α-HSDH.** The bound NADH and reaction product (7-oxoglycochenodeoxycholic acid) are shown in purple and blue, respectively. Protein atoms are colored green (carbon), red (oxygen), and blue (nitrogen). The catalytic residues (Tyr159, Ser146, and Lys163), substrate-binding residues (Val200, Leu254, and Asn151), and cofactor-binding residue (Asp42) are shown. This figure was produced with the program, MOLSCRIPT (*28*).

TABLE II. **Kinetic constants for the wild-type and mutant forms of the 7α-HSDH.**

	K_m (CA)[a] (mM)	K_m (NAD^+) (mM)	K_d (NAD^+) (mM)	k_{cat} (CA)[b] (s^{-1})	k_{cat}/K_m ($mM^{-1} \cdot s^{-1}$)	Comparative activity (%)
Wild-type	0.361	0.279	0.065	151	418	100
Y159F	N.A.[c]	N.A.	0.075	N.A.	N.A.	N.A.
Y159H	0.407	0.386	0.081	20.1	49.4	13.3
K163R	0.612	0.159	0.45	96.2	157	63.7
K163I	0.223	0.329	0.55	7.93	35.6	5.25
S146H	0.283	0.364	0.12	53.7	190	35.6
S146A	0.415	0.302	0.095	30.7	74.0	20.3

[a]CA, cholic acid. [b]A molecular weight of 107,112 was used for 7α-HSDH in the calculation. [c]No activity.

TABLE III. **X-ray crystallographic data and statistics for some mutants (ternary complexes).**

	Wild type[a]	Y159F	Y159H	K163R
Data collection statistics				
Unit cell dimensions (Å)				
a	81.66	81.75	82.09	81.85
b	81.66	81.75	82.09	81.85
c	214.6	214.9	215.6	216.0
Resolution	1.80	2.49	2.32	2.46
R_{merge}[b]	8.50	8.29	8.14	10.85
Observed reflections	221,323	87,851	92,067	86,842
Unique reflections	57,290	22,312	25,457	20,073
Refinement statistics				
Resolution range (Å)	8.0–1.8	8.0–2.49	8.0–2.32	8.0–2.46
Final *R*-factor[c]	0.207	0.182	0.189	0.190
rms dev. bond lengths (Å)	0.010	0.011	0.011	0.013
rms dev. bond angles (deg)	1.67	1.78	1.74	2.00

[a]Tanaka *et al.* (*6*). [b]$R_{merge}(I) = \Sigma h \Sigma i |\langle I(h) \rangle i - I(h)| / \Sigma h \Sigma i I(h) i$, where i represents different imaging plates. [c]R-factor $= \Sigma ||F_o| - k|F_c|| / \Sigma |F_o|$, where $|F_o|$ and $|F_c|$ are the observed and calculated structure factor amplitudes, respectively.

Refinement Procedure—The crystal structures of the mutants were solved by the difference Fourier method using the coordinates of the wild-type enzyme as the starting model. The mutant models were refined using the program, X-PLOR, for energy restraints and optional dynamics at high temperature. Forty cycles of positional refinement were carried out before the annealing procedure. Simulated annealing was carried out by setting the initial temperature at 600 K and applying gradual cooling to a final temperature of 300 K (*16*). After 20 cycles of *B*-factor refinement following the simulated annealing, the *R*-factor had decreased to 19.7% at 2.5 Å, 20.1% at 2.3 Å, and 19.5% at 2.5 Å for the ternary complexes of Y159F, Y159H, and K163R, respectively. At this stage, the $2F_o - F_c$ and $F_o - F_c$ electron density maps were calculated from the refined models, and the side-chain at each mutation site was replaced by the corresponding residue, using the program, TURBO-FRODO. These maps showed clear densities over the entire molecules. The water positions for each mutant were also defined by these maps by comparison with the wild-type water positions. Subsequent positional and *B*-factor refinement was performed for 15 cycles and 20 cycles, respectively. The final *R* factors for the ternary complexes of Y159F, Y159H, and K163R were 18.2% at 2.49 Å, 18.9% at 2.32 Å, and 19.0% at 2.46 Å. The binary complexes of the three mutants were also refined by the same procedure, and the final *R* factors for all mutants dropped below 20% (data not shown). Other refinement parameters for the ternary complex of each mutant are summarized in Table III.

The Structures of the Mutant Enzymes—There were little overall structural changes between the wild-type and mutant enzymes. The changes in electron density associated with the replaced amino acids were inspected with the

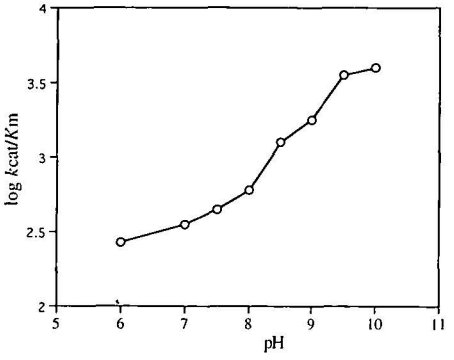

Fig. 4. **Effect of pH on the activity of the wild-type 7α-HSDH.** The k_{cat} and K_m values with cholic acid as the substrate were determined for the wild-type enzyme and plotted as $\log(k_{cat}/K_m)$ at the pH values indicated.

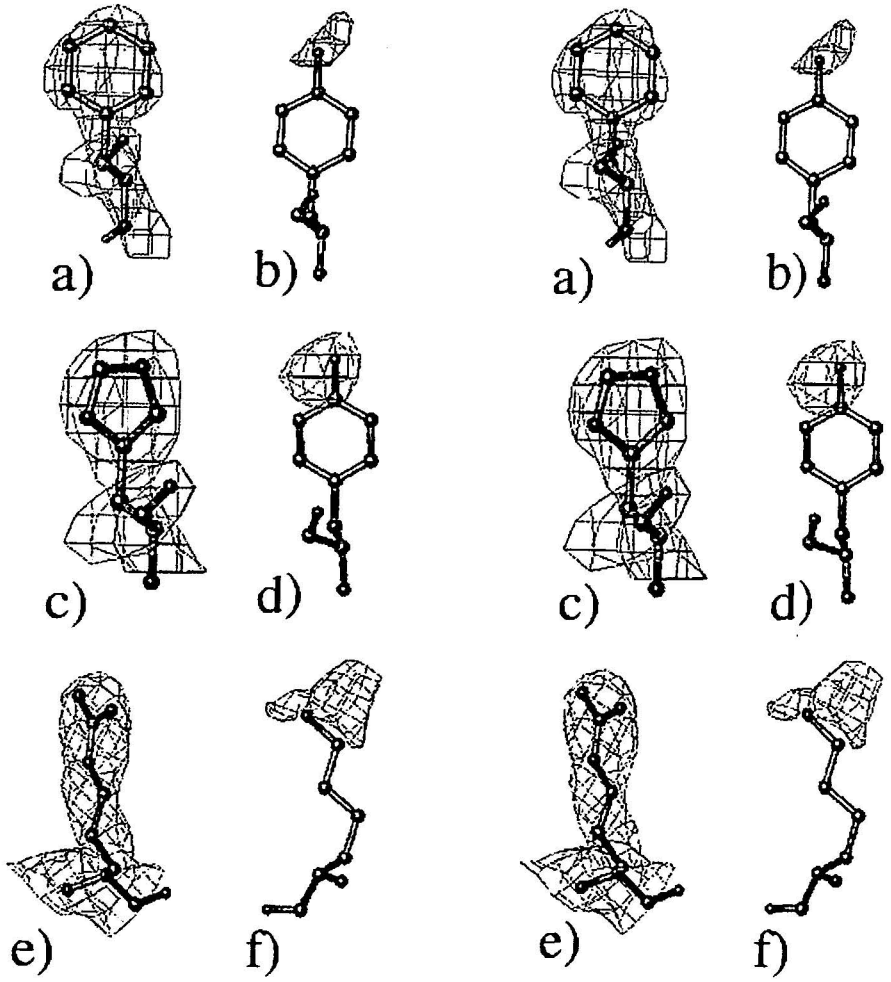

Fig. 3. **Representative portions of the electron density maps showing the changes in electron density associated with the replacement of amino acids.** a, c, and e are omit maps computed excluding the appropriate side chains from the wild-type model. b, d, and f are difference ($F_o - F_c$) maps computed with the mutant diffraction data and wild-type coordinates. (a) Y159F omit map. (b) Y159F $F_o - F_c$ map. (c) Y159H omit map. (d) Y159H $F_o - F_c$ map. (e) K163R omit map. (f) K163R $F_o - F_c$ map. The contour levels are 2.0 s (a, c, e, and f) and −2.0 s (b and d). These figures were produced with the program, TURBO-FRODO.

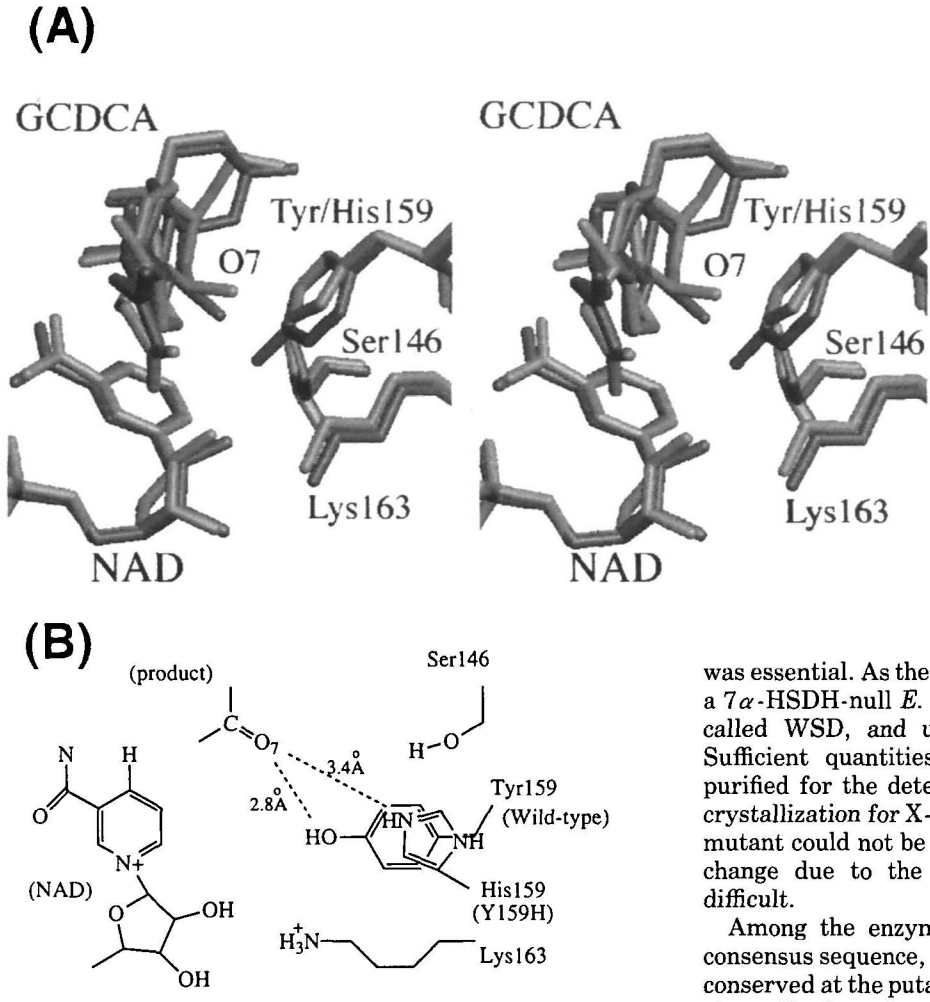

Fig. 5. **Superimpositioning the active site in the ternary complexes of the wild-type and Y159H mutant enzymes.** (A) Stereoview of the active site in the ternary complexes of the wild-type (gray) and Y159H (white). (B) Scheme illustrating the interaction between the O7 atom of the product and the side chain at position 159 in the wild-type and Y159H mutant enzymes.

$F_o - F_c$ and omit maps for each mutant. Figure 3a shows the Y159F 2.0 σ omit map for residue 159, removing the side chain of residue 159 estimated for Y159F. The positive density is supportive of the presence of phenylalanine at position 159. In addition, the Y159F $-2.0\ \sigma\ F_o - F_c$ map for residue 159 shows the large negative peak corresponds to the lack of density for a hydroxyl group (Fig. 3b). The $F_o - F_c$ map between the wild-type structure and the Y159H data (Fig. 3d) also shows a large negative peak similar to that in Fig. 3b. The omit map confirms that a histidine residue is present at this position (Fig. 3c). Figure 3f shows the K163R 2.0 $\sigma\ F_o - F_c$ map for residue 163. The positive peak in this figure corresponds to the guanidino group of arginine. The omit map also supports the presence of an arginine residue at position 163 (Fig. 3e).

Effect of pH on the Activity of the Wild-Type Enzyme—In order to determine the pK_a value for the wild-type enzyme, the K_m and k_{cat} values of the enzyme were determined at different pH values in the range of 6.0 to 10.0 with cholic acid as the substrate. As shown in Fig. 4, the pK_a value of the wild-type enzyme is 7.7.

DISCUSSION

In order to characterize the 7α-HSDH mutants in *E. coli*, elimination of the native-enzyme background in the cells was essential. As the first step in this study, we constructed a 7α-HSDH-null *E. coli* W3110 mutant strain, which was called WSD, and used it as the host for expression. Sufficient quantities of all the mutant enzymes were purified for the determination of kinetic parameters and crystallization for X-ray analysis. Nevertheless, the K163I mutant could not be crystallized, probably because a local change due to the mutation makes the crystallization difficult.

Among the enzymes belonging to the SDR family, a consensus sequence, Tyr-(Xaa)$_3$-Lys (X can be variable), is conserved at the putative active site (*17*). Some mutagenesis studies have been performed on these conserved tyrosine and lysine residues, which clearly showed that the conserved tyrosine residue is essential for the catalysis (*18-23*). In dihydropteridine reductase (DHPR), of which the crystal structure (binary complex with NADH) has been elucidated (*24*), the roles of these two residues were explained on the basis of the results of kinetic analysis and the crystal structures of various mutants (*25, 26*).

As shown in Fig. 2, Tyr159 and Lys163 in 7α-HSDH, which are equivalent to these residues in the Tyr-(Xaa)$_3$-Lys motif, are located around the substrate analogue in the ternary complex. To determine the roles of these two residues, we constructed a series of mutants that would have different chemical properties. First, we mutated tyrosine to phenylalanine, which lacks the hydroxyl group at the phenolic ring but is structurally similar to tyrosine. The Y159F mutant turned out to be inactive, although the active site in the binary and ternary complexes of this mutant is almost the same as the wild-type enzyme. This confirms the previous reports suggesting that the tyrosine residue is essential for catalysis as a catalytic base.

However, the Y159H mutant retained 13.3% of the wild-type enzyme activity. Since histidine is as good a proton donor as tyrosine, this result indicates that the histidine residue adopted a different conformation at the active site from that of the wild-type tyrosine residue. As shown in Fig. 5A, His159 interacted with the O7 atom of the substrate at a different position from that in the wild-type,

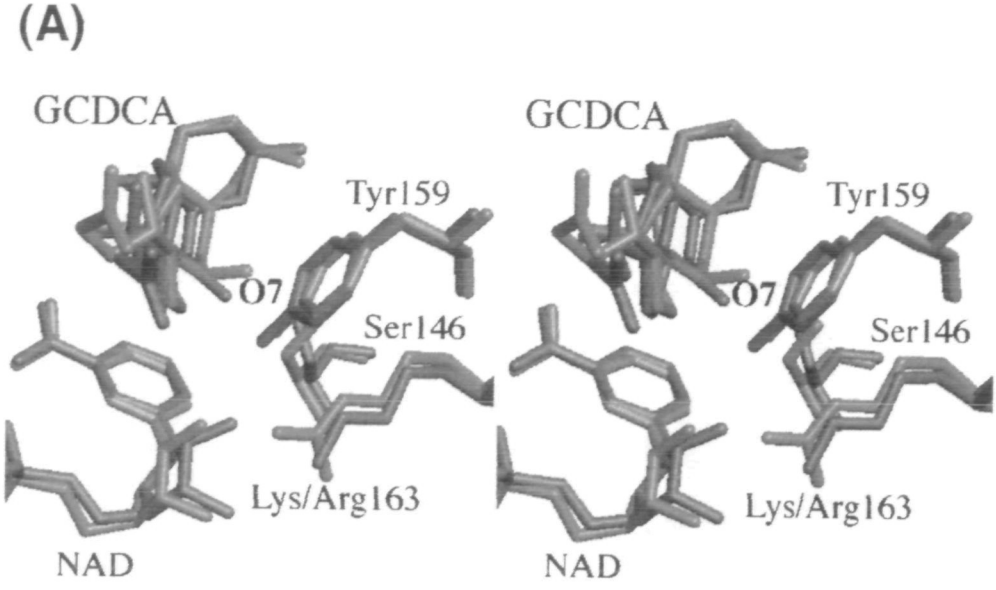

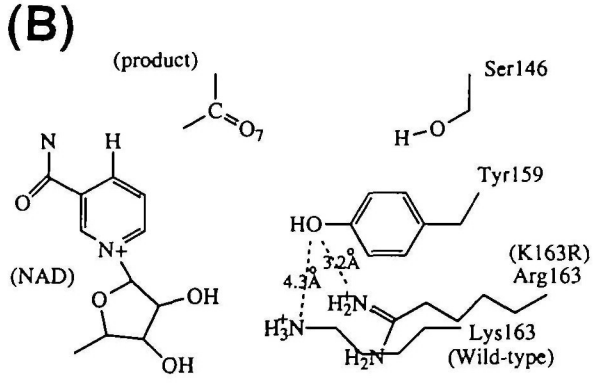

Fig. 6. **Superimpositioning the active site in the ternary complexes of the wild-type and K163R mutant enzymes.** (A) Stereoview of the active site in the ternary complexes of the wild-type (gray) and K163R (white) enzymes. (B) Scheme illustrating the interaction between the side chain of Tyr159 and the side chain at position 163 in the wild-type and K163R mutant enzymes.

although a striking conformation change was not observed in comparison with the wild-type enzyme. His159 in the Y159H mutant was hydrogen-bonded with the oxygen atom at position 7 of the substrate [NE2(His159)...O7(product): 3.4 Å], but the distance was greater than that in the wild-type [OH(Tyr159)...O7(product): 2.8 Å] (Fig. 5B). The Y146H mutant in DHPR exhibits a similar reduction in activity. One explanation for this result was that the angle of proton transfer by the His146 mutant is more deviated from the ideal value (*26*).

The strictly conserved Lys163 was found to form a hydrogen bond with the 2′,3′-hydroxyl group of the nicotinamide ribose of NAD^+ in both the binary and ternary complexes of the wild-type enzyme (Fig. 2). In the K163I mutant, the activity decreased dramatically (only 5.3% of the wild-type enzyme level), and binary complex (with NAD^+) crystals could not be obtained. This may be due to the incorrect orientation and binding of NADH due to the loss of hydrogen bonding to the nicotinamide ribose.

The K163R mutant showed a K_d value of as low as that of the K163I mutant. In the active site of the K163R complexes, movement of the nicotinamide ribose of NAD^+ was observed when compared with the wild-type complex (Fig. 6A). These results may infer that the unstable conformation of the nicotinamide ribose has some influence on the activity in the K163R mutant. However, this mutant retained comparatively high activity, showing 64% of the k_{cat} of the wild-type enzyme. This observation indicates that the guanidium group of arginine facilitates catalysis by the Tyr159 residue as the ε-amino group of Lys163 in the wild-type enzyme does. Actually, the distance between OH (Tyr159) and NH_2 (Arg163) in the K163R ternary complex (3.2 Å) was similar to that to NE (Lys163) in wild-type complex (4.3 Å) (Fig. 6B). From these results, we suggest that Lys163 may lower the pK_a value of the hydroxyl group of Tyr159.

Usually, the phenolic group of a tyrosine side chain has a pK_a value of 10.5. However, the pK_a value of the catalytic residue (Tyr159) was about 7.7. If Tyr159 is deprotonated on catalysis, its pK_a value must be lowered through the effect of a certain local environment. These findings indicate that Lys163 may in fact play this role. In the *Drosophila* alcohol dehydrogenase, a similar role for this lysine (Lys156) has been proposed (*21*).

In the active site of the ternary complex, Ser146, which is highly conserved in the SDR family, directly interacts with the oxygen atom at position 7 of the steroid skeleton of bile acid through a hydrogen bond. The substitution of Ala for Ser146 leads to a fair reduction in the activity, as in the S146H mutant. This result indicates that the hydrogen bonding of Ser146 to the O7 atom of the substrate was important for obtaining the ideal angle of proton transfer. In 3β/17β-hydroxysteroid dehydrogenase (3β/17β-HSDH), the S138A mutant showed an almost complete loss of enzymatic activity, but with the substitution by Thr the full activity was retained. These results indicate that an essential factor for catalysis is the ability of the side chain at position 138 to form a hydrogen bond (*27*). Therefore, we strongly suggest the concept that Ser146 together with the Tyr-$(Xaa)_3$-Lys motif form a catalytic triad (Ser146-Tyr159-Lys163 in 7α-HSDH).

The catalytic mechanism for 7α-HSDH, which is proposed on the basis of the crystallographic and enzymatic observations, can be described as follows. In the first step, the deprotonated phenolic group of Tyr159 forms a hydrogen bond with the hydroxyl group attached to position 7 of

the steroid skeleton of the substrate. In the second step, the deprotonated tyrosine residue acts as a catalytic base that extracts a hydrogen from the hydroxyl group of the substrate. Concomitantly, NAD^+ transfers a hydrogen liberated from position 7 of the steroid skeleton through the "B-face" of the nicotinamide ring at position 4.

In conclusion, site-directed mutagenesis and crystallographic studies, we could confirm the roles of the three residues located at the active site of the *E. coli* 7α-HSDH. Tyr159 plays the role of a basic catalyst, Lys163 plays roles in binding with NAD^+ and lowering the pK_a value of Tyr159, and Ser146 may give rise to the ideal orientation of proton transfer through the hydrogen bonding to the O7 atom of the substrate, the intermediate or the product.

REFERENCES

1. MacDonald, I.A., Williams, C.N., and Mahony, D.E. (1973) 7α-Hydroxysteroid dehydrogenase from *Escherichia coli* B: preliminary studies. *Biochim. Biophys. Acta* **309**, 243-253
2. Prebha, V., Gupta, M., Seiffge, D., and Gupta, K.G. (1990) Purification of 7α-hydroxysteroid dehydrogenase from *Escherichia coli* strain 080. *Can. J. Microbiol.* **36**, 131-135
3. Yoshimoto, T., Higashi, H., Kanatani, K., Xu, S.L., Nagai, H., Oyama, H., Kurazono, K., and Tsuru, D. (1991) Cloning and sequencing of the 7α-hydroxysteroid dehydrogenase gene from *Escherichia coli* HB101 and characterization of the expressed enzyme. *J. Bacteriol.* **173**, 2173-2179
4. Yoshimoto, T., Nagai., H., Ito, K., and Tsuru, D. (1993) Location of the 7α-hydroxysteroid dehydrogenase gene (*hdhA*) on the physical map of the *Escherichia coli* chromosome. *J. Bacteriol.* **175**, 5730
5. Jörnvall, H., Bahr-Lindstrom, H., Jany, K.-D., Ulmer, W., and Froschle, M. (1995) Short-chain dehydrogenases/reductases. *Biochemistry* **34**, 6003-6013
6. Tanaka, N., Nonaka, T., Tanabe, T., Yoshimoto, T., Tsuru, D., and Mitsui, Y. (1996) Crystal structures of the binary and ternary complexes of 7α-hydroxysteroid dehydrogenase from *Escherichia coli*. *Biochemistry* **35**, 7715-7730
7. Daws, T., Lim, C.-J., and Fuchs, J.A. (1989) In vitro construction of *gshB::kan* in *Escherichia coli* and use of *gshB::kan* in mapping the *gshB* locus. *J. Bacteriol.* **171**, 5218-5221
8. Bingham, R.J., Hall, K.S., and Slonczewski, J.L. (1990) Alkaline induction of a novel gene locus, *alx*, in *Escherichia coli*. *J. Bacteriol.* **172**, 2184-2186
9. Dower, W.J. (1988) High efficiency transformation of *Escherichia coli* by high voltage electroporation. *Nucleic Acids Res.* **16**, 6127-6145
10. Birnboim, H.C. and Doly, J. (1979) A rapid alkaline extraction procedure for screening recombinant plasmid DNA. *Nucleic Acids Res.* **7**, 1513-1523
11. Ho, S.N., Hunt, H.D., Horton, R.M., Pullen, J.K., and Pease, L.R. (1989) Site-directed mutagenesis by overlap extension using the polymerase chain reaction. *Gene* **77**, 51-59
12. Bradford, M.M. (1976) A rapid and sensitive method for the quantitation of microgram quantities of protein utilizing the principle of protein-dye binding. *Anal. Biochem.* **72**, 248-254
13. Stinson, R.A. and Holbrook, J.J. (1973) Equilibrium binding of nicotine amide nucleotides to lactate dehydrogenases. *Biochem. J.* **131**, 719-728
14. Tanaka, N., Nonaka, T., Yoshimoto, T., Tsuru, D., and Mitsui, Y. (1996) Crystallization and preliminary X-ray crystallographic studies of 7α-hydroxysteroid dehydrogenase from *Escherichia coli*. *Acta Crystallogr.* **D52**, 215-217
15. Brünger, A.T. (1992) *X-PLOR Version 3.1. A System for X-Ray Crystallograph and NMR*, Yale University Press, New Haven, CT
16. Brünger, A.T. and Krukowski, A. (1990) Slow-cooling protocols for crystallographic refinement by simulated annealing. *Acta Crystallogr.* **A46**, 585-593
17. Persson, B., Krook, M., and Jörnvall, H. (1991) Characteristics of short-chain alcohol dehydrogenases and related enzymes. *Eur. J. Biochem.* **200**, 537-543
18. Ensor, C.M. and Tai, H.H. (1991) Site-directed mutagenesis of the conserved tyrosine 151 of human placental NAD^+-dependent 15-hydroxyprostaglandin dehydrogenase yields a catalytically inactive enzyme. *Biochem. Biophys. Res. Commun.* **176**, 840-845
19. Albalat, R., Duarte, G., and Atrian, S. (1992) Protein engineering of *Drosophila* alcohol dehydrogenase. The hydroxyl group of Tyr152 is involved in the active site of the enzyme. *FEBS Lett.* **165**, 190-196
20. Obeid, J. and White, P.C. (1992) Tyr-179 and Lys-183 are essential for enzymatic activity of 11β-hydroxysteroid dehydrogenase. *Biochem. Biophys. Res. Commun.* **188**, 222-227
21. Chen, Z., Jiang, J.C., Lin, Z.G., Lee, W.R., Baker, M.E., and Chang, S.H. (1993) Site-specific mutagenesis of *Drosophila* alcohol dehydrogenase: evidence for involvement of tyrosine-152 and lysine-156 in catalysis. *Biochemistry* **32**, 3342-3346
22. Cols, N., Marfany, G., Atrian, S., and Gonzalez-Duarte, R. (1993) Effect of site-directed mutagenesis on conserved positions of *Drosophila* alcohol dehydrogenase. *FEBS Lett.* **319**, 90-94
23. Whitely, J.M., Xuong, N.H., and Varughese, K.I. (1993) in *Chemistry and Biology of Pteridines and Folates* (Ayling, J.E., Nair, M.G., and Baugh, C.M., eds.), pp. 115-121, Plenum, New York
24. Varughese, K.I., Skinner, M.M., Whiteley, J.M., Matthews, D.A., and Xuong, N.H. (1992) Crystal structure of rat liver dihydropteridine reductase. *Proc. Natl. Acad. Sci. USA* **89**, 6080-6084
25. Varughese, K.I., Xuong, N.H., Kiefer, P.M., Matthews, D.A., and Whiteley, J.M. (1994) Structural and mechanistic characteristics of dihydropteridine reductase: a member of the Tyr-$(Xaa)_3$-Lys-containing family of reductases and dehydrogenases. *Proc. Natl. Acad. Sci. USA* **91**, 5582-5586
26. Kiefer, P.M., Varughese, K.I., Su, Y., Xuong, N.-H., Chang, C.-F., Gupta, P., Bray, T., and Whiteley, J.M. (1996) Altered structural and mechanistic properties of mutant dihydropteridine reductases. *J. Biol. Chem.* **271**, 3437-3444
27. Oppermann, C.T.U., Filling, C., Berndt, D.K., Persson, B., Benach, J., Ladenstein, R., and Jörnvall, H. (1997) Active site directed mutagenesis of 3β/17β-hydroxysteroid dehydrogenase establishes differential effects on short-chain dehydrogenase/reductase reactions. *Biochemistry* **36**, 34-40
28. Kraulis, P.J. (1991) MOLSCRIPT: a program to produce both detailed and schematic plots of protein structures. *J. Appl. Crystallogr.* **24**, 946-950